Mathematical Biosciences 244 (2013) 58–67

Contents lists available at SciVerse ScienceDirect

Mathematical Biosciences

journal homepage: www.elsevier.com/locate/mbs

Two-dimensional transport analysis of transdermal drug absorption with a non-perfect sink boundary condition at the skin-capillary interface

Laurent Simon [a,*], Juan Ospina [b]

[a] Otto H. York Department of Chemical, Biological and Pharmaceutical Engineering, New Jersey Institute of Technology, Newark, NJ 0702, USA
[b] Logic and Computation Group, Physics Engineering Program, School of Sciences and Humanities, EAFIT University, Medellin, Colombia

ARTICLE INFO

Article history:
Received 21 October 2011
Received in revised form 24 February 2013
Accepted 15 April 2013
Available online 26 April 2013

Keywords:
Laplace transform
Time constant
Partial differential equations
Percutaneous absorption
Two-dimensional diffusion

ABSTRACT

A transient percutaneous drug absorption model was solved in two dimensions. Clearance of the topically-applied pharmaceutical occured at the skin-capillary boundary. Timolol penetration profiles in the dermal tissue were produced revealing concentration gradients in the directions normal and parallel to the skin surface. Ninety-eight percent of the steady-state flux was reached after 85 h or four time constants. The analytical solution procedure agreed with published results. As the clearance rate increased relative to diffusion, the delivery rate and amount of drug absorbed into the bloodstream increased while the time to reach the equilibrium flux decreased. Researchers can apply the closed-form expressions to simulate the process, estimate key parameters and design devices that meet specific performance requirements.

1. Introduction

Currently, skin permeation may be evaluated using radioactive materials, tape stripping techniques or the label-free stimulated Raman scattering [1]. The mathematical modeling of percutaneous drug transport mechanisms has been a major area of research [2,3]. It can provide an accurate picture of the evolution of active pharmaceutical ingredients (APIs) after applying a patch, thus elucidating the role of enhancers in promoting diffusion through different skin layers.

One-dimensional (1-D) analyses are routinely conducted to portray the events occurring in the skin after application or removal of the delivery system [2,4]. Although these efforts do not incorporate the complexity of the skin structure, they serve as a basis for estimating physicochemical properties from experimental data. Even more elaborate two-pathway transdermal models, which included transcellular and intercellular phases of the stratum corneum and viable epidermis, were developed using transport perpendicular to the skin surface [5]. In the latter framework, transfer of species within the two phases can be explained. However, the level of details is still very low and fails to consider variations of the drug concentrations in the lateral direction. A two-dimensional (2-D) approach would help overcome some of these impediments and offer a profound insight into the mechanism governing transdermal absorption.

In response to the lack of 2-D depictions of percutaneous drug absorption, some researchers have introduced models based on kinetics generated from 1-D release data. George et al. proposed a 2-D mathematical construct to explain the influences of drug diffusivity and clearance, at the skin-capillary interface, on the delivery rate and the cumulative amount of drug released [6]. Using a finite-difference method to approximate the drug concentration, they were able to gather spatial information that would not have been possible with a 1-D model. The non-linear kinetic behavior of drugs, such as scopolamine and timolol, was later incorporated in a 2-D model proposed to describe a dual-sorption mechanism [7]. The theory suggests that, upon dermal application of a drug, some molecules dissolve and become available for diffusion while a fraction binds to sites in the skin. Again, a more comprehensive depiction of the process was achieved by including more than one molecular transport direction.

To date, published contributions have focused mainly on numerical solution techniques to track concentration profiles in a 2-D system [6,7]. In the absence of a closed-from solution, design parameters, such as the time required to reach a steady-state flux, were read from the plots. Similarly, the effects of the clearance and diffusion on the delivery rate were deduced from the graphs. The development of an analytical platform would make available, to researchers, expressions relating the equilibrium delivery rate, for example, to the model parameters. Suggestions on how to conduct experiments and analyze laboratory data in order to extract useful parameters may be provided. Research on multi-dimensional analytical solutions of transdermal delivery systems is necessary to start

* Corresponding author. Tel.: +1 973 596 5263; fax: +1 973 596 8436.
E-mail address: laurent.simon@njit.edu (L. Simon).

0025-5564/$ - see front matter © 2013 Elsevier Inc. All rights reserved.
http://dx.doi.org/10.1016/j.mbs.2013.04.004

building such a foundation. In this context, a closed-form solution to the model, presented in [6], is introduced. The concentration, flux and cumulative amount of drug released are derived. An effective time constant, which denotes the time it takes to attain a steady-state flux, is determined.

2. Transdermal delivery model

A patch of length h_c containing a medication is applied to the skin (Fig. 1). The drug concentration in the reservoir (c_b) remains constant during the treatment. Two segments perpendicular to the skin surface, h_u and h_d, are selected. The model assumes no exchange of material with the surroundings except at the skin-capillary boundary where a first-order elimination kinetics is observed. A mathematical representation of the process is given below [6]:

$$\frac{\partial c}{\partial t} = D\left(\frac{\partial^2 c}{\partial x_1^2} + \frac{\partial^2 c}{\partial x_2^2}\right) \tag{1}$$

$$\frac{\partial c(0, x_2, t)}{\partial x_1} = 0, \quad -h_d \leqslant x_2 < 0 \tag{2}$$

$$c(0, x_2, t) = c_b, \quad 0 \leqslant x_2 \leqslant h_c \tag{3}$$

$$\frac{\partial c(0, x_2, t)}{\partial x_1} = 0, \quad h_c < x_2 \leqslant h_c + h_u \tag{4}$$

$$\frac{\partial c(x_1, -h_d, t)}{\partial x_2} = 0, \quad 0 \leqslant x_1 \leqslant l_s \tag{5}$$

$$\frac{\partial c(x_1, h_c + h_u, t)}{\partial x_2} = 0, \quad 0 \leqslant x_1 \leqslant l_s \tag{6}$$

$$-D\frac{\partial c(l_s, x_2, t)}{\partial x_1} = K_{cl} c(l_s, x_2, t), \quad -h_d \leqslant x_2 \leqslant h_c + h_u \tag{7}$$

where D and K_{cl} are the drug diffusivity and clearance, at the skin-capillary boundary and l_s is the skin thickness. The vehicle/skin partition coefficient is one. Initially, the skin is free of the drug:

$$c(x_1, x_2, 0) = 0 \tag{8}$$

By using the following dimensionless variables:

$$x = \frac{x_1}{l_s}, \quad y = \frac{x_2}{l_s}, \quad \tau = \frac{tD}{l_s^2}, \quad C = \frac{c}{c_b}, \quad w = \frac{l_s K_{cl}}{D},$$
$$L_d = \frac{h_d}{l_s}, \quad L_c = \frac{h_c}{l_s}, \quad L_u = \frac{h_c + h_u}{l_s} \tag{9}$$

Eqs. (1)–(8) become

$$\frac{\partial C}{\partial \tau} = \frac{\partial^2 C}{\partial x^2} + \frac{\partial^2 C}{\partial y^2} \tag{10}$$

$$\frac{\partial C(0, y, \tau)}{\partial x} = 0, \quad -L_d \leqslant y < 0 \tag{11}$$

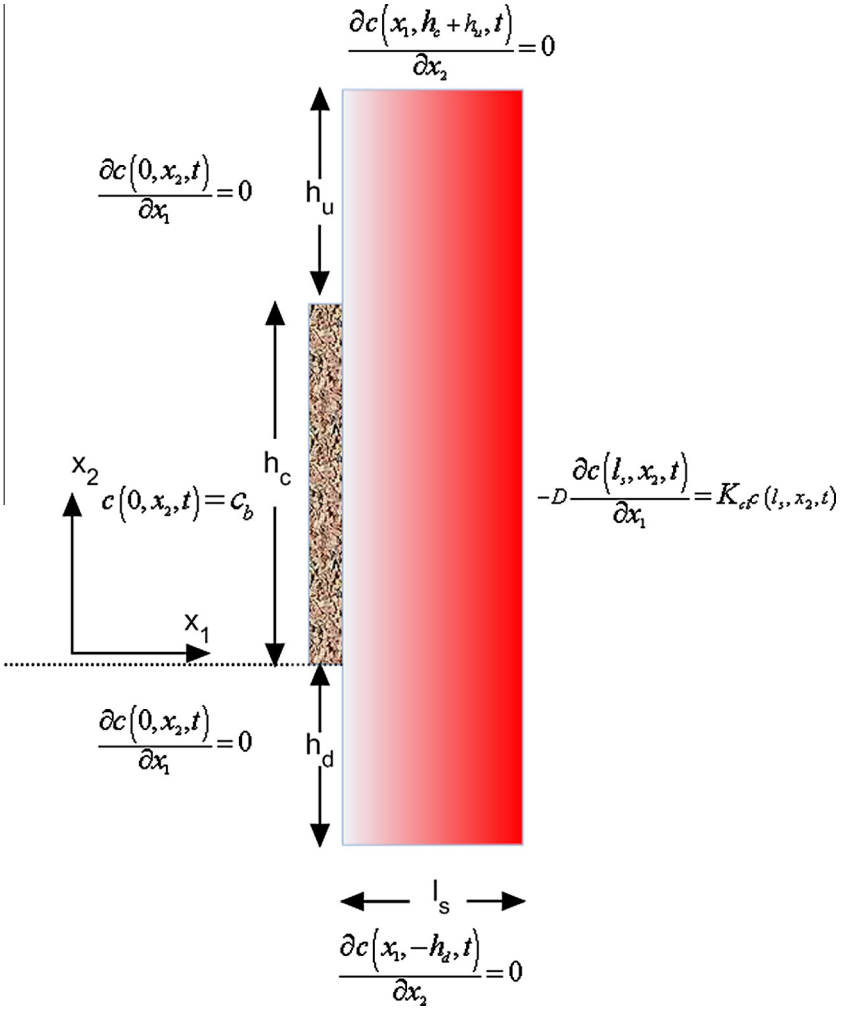

Fig. 1. Schematic of the percutaneous drug absorption model.

$$C(0,y,\tau)=1,\quad 0\leqslant y\leqslant L_c \tag{12}$$

$$\frac{\partial C(0,y,\tau)}{\partial x}=0,\quad L_c<y\leqslant L_u \tag{13}$$

$$\frac{\partial C(x,-L_d,\tau)}{\partial y}=0,\quad 0\leqslant x\leqslant 1 \tag{14}$$

$$\frac{\partial C(x,L_u,\tau)}{\partial y}=0,\quad 0\leqslant x\leqslant 1 \tag{15}$$

$$\frac{\partial C(1,y,\tau)}{\partial x}+wC(1,y,\tau)=0,\quad -L_d\leqslant y\leqslant L_u \tag{16}$$

$$C(x,y,0)=0 \tag{17}$$

3. Analytical solution

3.1. Concentration profile

A Laplace transform-based procedure is used to solve the problem. First, the boundary conditions (11)–(13) are combined into a single equation:

$$\left.\frac{\partial}{\partial x}C(x,y,\tau)\right|_{x=0}=\left.\left(\frac{\partial}{\partial x}C(x,y,\tau)+C(x,y,\tau)-1\right)\right|_{x=0}(\text{Heaviside}(y)-\text{Heaviside}(y-L_c)) \tag{18}$$

where "Heaviside$(y-a)$" is the step function defined as

$$\text{Heaviside}(y-a)=\begin{cases}1 & a\leqslant y\\ 0 & \text{otherwise}\end{cases} \tag{19}$$

It can be shown that the Laplace transform of $C(x,y,\tau)$, labeled $\bar{C}(x,y,s)$, is (see the Appendix for details)

$$\bar{C}(x,y,s)=\bar{C}_1(x,y,s)+\bar{C}_2(x,y,s) \tag{20}$$

where

$$\bar{C}_1(x,y,s)=-\frac{\left(e^{x\sqrt{s}}\sqrt{s}-e^{x\sqrt{s}}w+\sqrt{s}e^{-(x-2)\sqrt{s}}+we^{-(x-2)\sqrt{s}}\right)A_0}{\sqrt{s}-w} \tag{21}$$

and

$$\bar{C}_2(x,y,s)=\sum_{n=1}^{\infty}\left[-\frac{A_n\left(-e^{G_n x}G_n+e^{G_n x}w-e^{-G_n(x-2)}G_n-e^{-G_n(x-2)}w\right)\cos\left(\frac{n\pi(y+L_d)}{L_u+L_d}\right)}{-G_n+w}\right] \tag{22}$$

with

$$G_n=\sqrt{\frac{n^2\pi^2}{(L_u+L_d)^2}+s} \tag{23}$$

The amplitudes A_0 and A_n are determined by solving the system of Eqs. (24) and (27):

$$A_0=\frac{F_1}{F_2} \tag{24}$$

where the numerator and denominator of Eq. (24) are given by

$$F_1=\left\{\begin{array}{l}\left[\sum_{n=1}^{\infty}\frac{i_{1,n}A_nG_n\left(-G_n+w+e^{2G_n}G_n+e^{2G_n}w\right)}{-G_n+w}\right]s\\ +\left[\sum_{n=1}^{\infty}-\frac{i_{1,n}A_n\left(G_n-w+e^{2G_n}G_n+e^{2G_n}w\right)}{-G_n+w}\right]s-L_c\end{array}\right\}(w-\sqrt{s}) \tag{25}$$

and

$$F_2=s\left\{\begin{array}{l}L_us-\sqrt{s}L_uw+L_ds-\sqrt{s}L_dw-e^{2\sqrt{s}}sL_u-e^{2\sqrt{s}}sL_d-e^{2\sqrt{s}}\sqrt{s}L_uw\\ -e^{2\sqrt{s}}\sqrt{s}L_dw-L_cs+L_c\sqrt{s}w+L_cse^{2\sqrt{s}}+L_c\sqrt{s}e^{2\sqrt{s}}w-L_c\sqrt{s}+L_cw\\ -L_ce^{2\sqrt{s}}\sqrt{s}-L_ce^{2\sqrt{s}}w\end{array}\right\} \tag{26}$$

respectively, and

$$\begin{aligned}&-\left(\frac{1}{2}L_u+\frac{1}{2}L_d\right)\left(A_mG_m-\frac{A_mG_m(G_m+w)e^{2G_m}}{G_m-w}\right)\\ &=\frac{A_0T_m(L_u+L_d)\left(-s+se^{2\sqrt{s}}+\sqrt{s}w+\sqrt{s}e^{2\sqrt{s}}w\right)}{m\pi\left(\sqrt{s}-w\right)}\\ &\quad+\sum_{n=1}^{\infty}i_{1,n,m}\left(A_nG_n-\frac{A_nG_n(G_n+w)e^{2G_n}}{G_n-w}\right)\\ &\quad-\frac{A_0T_m(L_u+L_d)\left(e^{2\sqrt{s}}\sqrt{s}+e^{2\sqrt{s}}w+\sqrt{s}-w\right)}{m\pi(\sqrt{s}-w)}\\ &\quad+\sum_{n=1}^{\infty}i_{1,n,m}\left(A_n+\frac{A_n(G_n+w)e^{2G_n}}{G_n-w}\right)-\frac{(L_u+L_d)T_m}{sm\pi}\end{aligned} \tag{27}$$

in which $m=1,2,\ldots,\infty$.

The coefficients $i_{1,n}$, $i_{1,n,m}$ and T_m are

$$i_{1,n}=\int_{-L_d}^{L_u}\left[-\cos\left(\frac{n\pi(y+L_d)}{L_u+L_d}\right)(\text{Heaviside}(y)-\text{Heaviside}(y-L_c))\right]dy \tag{28}$$

$$i_{1,n,m}=\int_{-L_d}^{L_u}\left[-\cos\left(\frac{n\pi(y+L_d)}{L_u+L_d}\right)\cos\left(\frac{m\pi(y+L_d)}{L_u+L_d}\right)(\text{Heaviside}(y)-\text{Heaviside}(y-L_c))\right]dy \tag{29}$$

and

$$\begin{aligned}T_m=&-\sin\left(\frac{\pi mL_d}{L_u+L_d}\right)+\sin\left(\frac{\pi mL_c}{L_u+L_d}\right)\cos\left(\frac{\pi mL_d}{L_u+L_d}\right)\\ &+\cos\left(\frac{\pi mL_c}{L_u+L_d}\right)\sin\left(\frac{\pi mL_d}{L_u+L_d}\right)\end{aligned} \tag{30}$$

3.2. Delivery rate

A dimensionless transdermal flux is defined by

$$J(\tau)=-\int_{-L_d}^{L_u}\left.\frac{\partial}{\partial x}C(x,y,\tau)\right|_{x=1}dy \tag{31}$$

or

$$J(\tau)=w\int_{-L_d}^{L_u}C(x=1,y,\tau)dy \tag{32}$$

by using Eq. (16). The Laplace transform of Eq. (32) is

$$\bar{J}(s)=w\int_{-L_d}^{L_u}\bar{C}(x=1,y,s)dy \tag{33}$$

Given the concentration $\bar{C}(x=1,y,s)$ from Eqs. (20) and (33) becomes

$$\bar{J}(s)=\frac{F_3}{F_2} \tag{34}$$

where

$$F_3=2w(L_u+L_d)e^{\sqrt{s}}\sqrt{s}\left\{\begin{array}{l}\left[\sum_{n=1}^{\infty}\frac{i_{1,n}A_nG_n\left(-G_n+w+e^{2G_n}G_n+e^{2G_n}w\right)}{-G_n+w}\right]s\\ +\left[\sum_{n=1}^{\infty}-\frac{i_{1,n}A_n\left(G_n-w+e^{2G_n}G_n+e^{2G_n}w\right)}{-G_n+w}\right]s-L_c\end{array}\right\} \tag{35}$$

and F_2 is given by Eq. (26). The flux $J(\tau)$ is obtained by inverting Eq. (34).

3.3. Cumulative amount of drug released

The normalized cumulative amount of drug released at time τ is defined by

$$M(\tau) = \int_0^\tau \frac{J(\sigma)}{J(\infty)} d\sigma \tag{36}$$

and is calculated once an expression for $J(\tau)$ is available.

3.4. Effective time constant

The effective relaxation time (or time constant) is defined by [8,9]

$$t_{eff} = \int_0^\infty t\Omega(t)dt \tag{37}$$

where $\Omega(t)$ represents a probability density function:

$$\Omega(t) = \frac{(g_e - g(t))}{\int_0^\infty (g_e - g(t))dt} \tag{38}$$

It can be shown that Eq. (37) is equivalent to

$$t_{eff} = \lim_{s\to 0}\left(\frac{\psi_{ss}}{s^2} + \frac{d\bar{\psi}(s)}{ds}\right)\left[\lim_{s\to 0}\left(\frac{\psi_{ss}}{s} - \bar{\psi}(s)\right)\right]^{-1} \tag{39}$$

where $\bar{\psi}$ is the Laplace transform of ψ and ψ_{ss} is its equilibrium value. If the normalized flux is considered (i.e., $\psi = J(\tau)/J(\infty)$ and $\psi_{ss} = 1$), the dimensionless time constant is

$$\tau_{eff} = \lim_{s\to 0}\left(\frac{1}{s^2} + \frac{d}{ds}\left(\frac{\bar{J}(s)}{J(\infty)}\right)\right)\left[\lim_{s\to 0}\left(\frac{1}{s} - \frac{\bar{J}(s)}{J(\infty)}\right)\right]^{-1} \tag{40}$$

3.5. CAS analysis and computational implementation

Symbolic manipulations were conducted with the CAS system Maple by Waterloo Sofware, version 12 (OS version: Microsoft Windows XP Professional Version 2002, Service Pack 2; Machine: Genuine intel (R) CPU T 2080 1.73 Ghz 795 Mhz). The "*PDEtools*" package, a set of routines, was used to derive the analytical solution. The following steps were carried out:

- Write the original partial differential equation, with the initial conditions, in the Laplace domain.
- Solve the transformed partial differential equation to obtain $\bar{C}(x,y,s)$, the Laplace transform of $C(x,y,t)$. It was first assumed that $\bar{C}(x,y,s)$ could be expressed in terms of a product: $\bar{C}(x,y,s) = f(x,s).g(y,s)$.
- Expand $\bar{C}(x,y,s)$ as a Fourier series.
- Apply the boundary conditions and compute the coefficients of the Fourier series using orthogonality properties of trigonometric functions.
- Write the inverse Laplace transform of the resulting Fourier series as a Bromwich integral.
- Compute the Bromwich integral using the residue theorem.

In addition to "*PDEtools*", the following routines were used: "*VectorCalculus*", to compute the Laplacian of a function; "*inttrans*", to perform integral transformation and obtain Laplace transforms; and "*plots*", to draw the two-dimensional concentration profiles. The rest of the graphics were generated in Mathematica (Wolfram Research, Inc.). The Bromwich integral, which is not readily available in Maple, was computed using the residue theorem. The residues were calculated using either the command *residue* or formulas implemented in Maple.

4. Zero-order solution

4.1. Concentration profile

A zero-order solution can be obtained by setting $A_n = 0$ with $n = 1, 2, \ldots, \infty$. In this case, Eq. (20) reduces to

$$\bar{C}(x,y,s) = -\frac{\left(e^{2x\sqrt{s}}\sqrt{s} - e^{2x\sqrt{s}}w + \sqrt{s}e^{2\sqrt{s}} + e^{2\sqrt{s}}w\right)L_c e^{-x\sqrt{s}}}{F_2} \tag{41}$$

Using the residue theorem, the inverse Laplace transform of the zero-order approximation of $\bar{C}(x,y,s)$ is

$$C(x,y,\tau) = -\frac{L_c(-w + xw - 1)}{L_d w + L_u w + L_c} + \sum_{p=1}^{\infty}\left[-\frac{\left(\frac{1}{2}je^{\alpha_p xj}\alpha_p - e^{\alpha_p xj}w + \frac{1}{2}je^{\alpha_p j}\alpha_p + e^{\alpha_p j}w\right)L_c e^{-\frac{1}{2}\alpha_p xj}e^{-\frac{1}{2}\alpha_p^2\tau}}{\left(\frac{\partial F_2}{\partial s}\right)\Big|_{s=-\frac{1}{4}\alpha_p^2}}\right] \tag{42}$$

where j is an imaginary number and α_p are such that $-\frac{1}{4}\alpha_p^2$ are the zeros of F_2. It is worthwhile to note that the zero-order approximation is independent of y.

4.2. Delivery rate

With $A_n = 0$ and $n = 1, 2, \ldots, \infty$, Eq. (34) reduces to

$$\bar{J}(s) = -\frac{2we^{\sqrt{s}}\sqrt{s}L_c(L_u + L_d)}{F_2} \tag{43}$$

The steady-state flux is derived by applying the final value theorem:

$$J(\infty) = \frac{L_c w(L_u + L_d)}{L_d w + L_u w + L_c} \tag{44}$$

As a result,

$$\frac{\bar{J}(s)}{J(\infty)} = -\frac{2e^{\sqrt{s}}\sqrt{s}(L_d w + L_u w + L_c)}{F_2} \tag{45}$$

The inverse Laplace transform of Eq. (45) leads to

$$\frac{J(\tau)}{J(\infty)} = 1 - 2\sum_{p=1}^{\infty}\frac{(L_d w + L_u w + L_c)e^{\left(-\frac{1}{4}\alpha_p^2\tau\right)}}{\left[\frac{\partial}{\partial s}\left(\frac{F_2}{\sqrt{s}e^{\sqrt{s}}}\right)\right]\Big|_{s=-\frac{1}{4}\alpha_p^2}} \tag{46}$$

4.3. Cumulative amount of drug released

The zero-order approximation of $M(\tau)$ is obtained from Eq. (46):

$$M(\tau) = \tau + 8\sum_{p=1}^{\infty}\frac{(L_d w + L_u w + L_c)\left[e^{\left(-\frac{1}{4}\alpha_p^2\tau\right)} - 1\right]}{\alpha_p^2\left[\frac{\partial}{\partial s}\left(\frac{F_2}{\sqrt{s}e^{\sqrt{s}}}\right)\right]\Big|_{s=-\frac{1}{4}\alpha_p^2}} \tag{47}$$

4.4. Effective time constant

Using $A_n = 0$ and $n = 1, 2, \ldots, \infty$, Eq. (40) takes the form

$$\tau_{eff} = \frac{P_1}{P_2} \tag{48}$$

where

$$\begin{aligned} P_1 = {} & -40L_c^2w^2 + 108L_d w^2 L_c + 108L_u w^2 L_c - 300L_d^2 w \\ & - 132L_c^2 w + 420L_d L_c - 75L_u^2 w^2 - 600L_u L_d w - 75L_d^2 w^2 \\ & + 420L_u L_c - 720L_u L_d - 300L_u^2 w - 360L_u^2 - 360L_d^2 \\ & - 150L_d w^2 L_u + 390L_c w L_u + 390L_c w L_d - 135L_c^2 \end{aligned} \tag{49}$$

and

$$P_2 = 60(-3L_d w - 3L_u w + 3L_c - 6L_u + 2L_c w - 6L_d)(L_d w + L_u w + L_c) \quad (50)$$

From Eq. (48), limit cases, corresponding to low- and high-clearance drugs (i.e., $w = 0$, $w \to \infty$, respectively), are derived:

$$\lim_{w\to\infty} \tau_{eff} = -\frac{1}{60} \times \frac{40L_c^2 - 108L_dL_c - 108L_uL_c + 75L_u^2 + 75L_d^2 + 150L_uL_d}{(-3L_d - 3L_u + 2L_c)(L_u + L_d)} \quad (51)$$

and

$$\lim_{w\to 0} \tau_{eff} = -\frac{1}{12} \times \frac{24L_d^2 - 28L_dL_c + 48L_uL_d + 9L_c^2 - 28L_uL_c + 24L_u^2}{(-2L_d + L_c - 2L_u)L_c} \quad (52)$$

With $L_u > L_c$, the following inequality is achieved:

$$\lim_{w\to\infty} \tau_{eff} < \lim_{w\to 0} \tau_{eff} \quad (53)$$

which is an important result provided by the zero-order approximation. This finding suggests that it takes less time to attain a steady-state flux if the clearance at the skin-capillary interface is very large compared to a low drug absorption into the blood stream. Equation (53) is in line with published numerical studies using the same model [6]. By defining w as $w = (1 - r)/r$, George et al. observed that the period elapsed before reaching $J(\infty)$ was shorter as r decreased.

5. First-order solution

5.1. Concentration profile

A first-order approximation is developed to improve the accuracy of the zero-order estimation. The enhanced solution would allow researchers to visualize how the drug concentration changes in the x- and y- directions. The coefficient A_n is set equal to zero for all $n = 2, 3, \ldots, \infty$. As a result,

$$\bar{C}(x,y,s) = -\frac{A_0\left(e^{x\sqrt{s}}\sqrt{s} - e^{x\sqrt{s}}w + \sqrt{s}e^{-(x-2)\sqrt{s}} + we^{-(x-2)\sqrt{s}}\right)}{\sqrt{s} - w} - \frac{A_1\left(-e^{G_1 x}G_1 + e^{G_1 x}w - e^{-G_1(x-2)}G_1 - e^{-G_1(x-2)}w\right)\cos\left(\frac{\pi(y+L_d)}{L_u+L_d}\right)}{-G_1 + w} \quad (54)$$

Closed-form representations for A_0 and A_1 are determined from Eqs. (24) and (27). These expressions are not reported in this work because of page limitations. The concentration $C(x,y,\tau)$ is found by inverting Eq. (54).

5.2. Delivery rate

A first-order approximation of Eq. (35) leads to the following expression:

$$\bar{J}(s) = \frac{2w(L_u + L_d)e^{\sqrt{s}}\sqrt{s}}{F_2}\left\{\begin{array}{l}\left[\frac{i_{1,1}A_1G_1(-G_1+w+e^{2G_1}G_1+e^{2G_1}w)}{-G_1+w}\right]s \\ -\left[\frac{i_{1,1}A_1(G_1-w+e^{2G_1}G_1+e^{2G_1}w)}{-G_1+w}\right]s - L_c\end{array}\right\} \quad (55)$$

The flux $J(\tau)$ is obtained by taking the inverse Laplace transform of Eq. (55).

5.3. Cumulative amount of drug released

The Laplace transform of the normalized cumulative amount of drug released is derived from Eq. (55):

$$\bar{M}(s) = \frac{1}{sJ(\infty)}\frac{2w(L_u + L_d)e^{\sqrt{s}}\sqrt{s}}{F_2}\left\{\begin{array}{l}\left[\frac{i_{1,1}A_1G_1(-G_1+w+e^{2G_1}G_1+e^{2G_1}w)}{-G_1+w}\right]s \\ -\left[\frac{i_{1,1}A_1(G_1-w+e^{2G_1}G_1+e^{2G_1}w)}{-G_1+w}\right]s - L_c\end{array}\right\} \quad (56)$$

by applying the integral formula $\bar{M}(s) = [\bar{J}(s)/J(\infty)]/s$ where $J(\infty)$ is calculated using the final value theorem. The profile $M(\tau)$ is created by inverting Eq. (56).

5.4. Effective time constant

It is possible to derive an analytical expression for the effective time constant. However, the formula is not presented in this contribution because of space limitations. As in the case of $\bar{M}(s)$, the ratio $\bar{J}(s)/J(\infty)$ is calculated from Eq. (55).

6. Results and discussions

6.1. Permeation of timolol

The model parameters for the beta-adrenoceptor blocking agent, timolol, were used in this work. Previous studies show that absorption of the drug can be represented by Eq. (70) [3]. The diffusivity through a cadaver skin of thickness 15 μm is 1.14×10^{-11} cm^2/s [10]. Values for L_c, L_d and L_u were obtained from [6] and the remaining data came from [3] (See Table 1). Fig. 2 shows the concentration profile in the skin when the first-order estimation was implemented. Over time, an increasing number of molecules penetrated the skin. The highest API level was detected at the vehicle/skin boundary and a concentration gradient was maintained across the skin as predicted by Fick's law. Fig. 3 describes the cumulative amount of timolol released into the blood using zero- and first-order approximations. The difference between the two estimations was imperceptible. Both methods gave t_{eff} = 21.24 h. As observed in previous results [9], 98% of the flux was achieved at $4t_{eff}$ (Fig. 4). This measure can be helpful in designing devices that meet user-defined requirements.

6.2. Effects of w on τ_{eff} and $M(\tau)$

The influences of w on the time to reach a steady-state flux value and the cumulative amount of drug released were investigated by George et al. [6]. These studies were repeated here to show that the analytical solution, presented in this contribution, led to the results reported in the numerical approach. In addition, the effects of w on τ_{eff} were now captured through a mathematical expression. Values for L_c, L_d and L_u corresponded to those listed in Table 1 [6]. The w numbers selected were gathered from the r range given in the original publication (i.e., $w = (1 - r)/r$). Based on Figs. 5 and 6, both the flux and cumulative amount of drug released increase with the clearance. The effective time constant decreases with a rise in w (Fig. 7). As the absorption rate increases, a larger concentration difference is established across the skin, leading to a higher flux, in accordance with Fick's laws of diffusion, in a relatively short time.

With the two-dimensional analysis, a more accurate picture of drug concentration profiles in the skin can be achieved. Contrary to a numerical approach, stability is not a concern. Closed-form

Table 1
Model parameters for the transdermal delivery of timolol.

l_s (cm)	c_b (μg/cm^3)	K_{cl} (cm/h)	D (cm^2/h)	h_c (cm)	h_d (cm)	h_u (cm)
0.0015	200,000	1.5	4.104E−08	0.00075	0.00375	0.00375
L_c	L_d	L_u	w			
0.5	2.5	3	54,825			

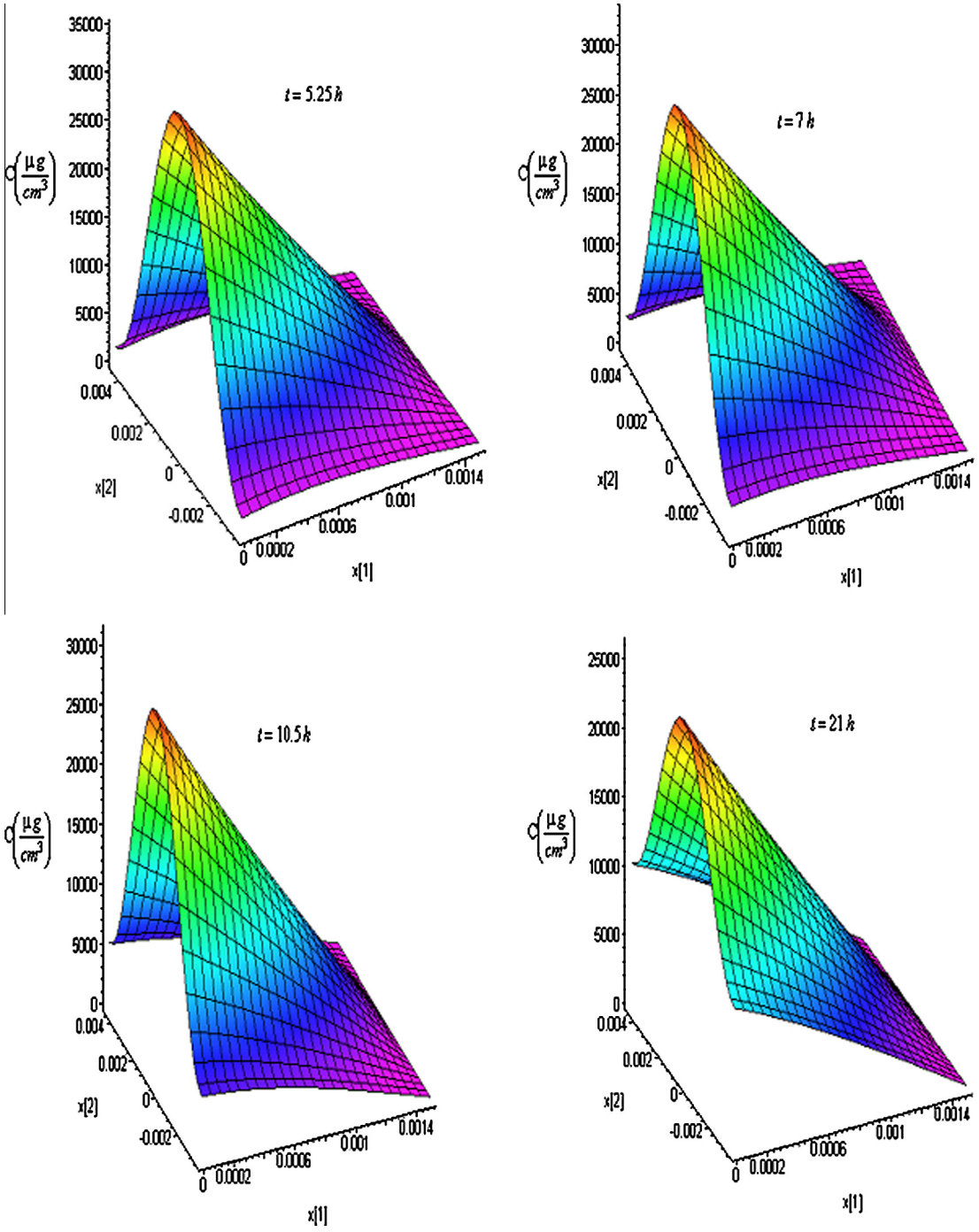

Fig. 2. Two-dimensional concentration distributions of timolol in the skin at various times. The first-order solution was used.

expressions for $M(\tau)$ and $J(\tau)/J(\infty)$ allow researchers to simulate the process without prior knowledge of how to solve partial differential equations efficiently. The analytical results obtained with Maple led to the derivation of an effective time constant in terms of properties of the patch and formulation. This parameter can be used to study the effect of design variables of controlled-release devices on the time elapsed to reach a steady-state delivery rate. In addition, the solution method can be implemented in software environments that do not offer suitable procedures to solve PDE problems in two dimensions. The code written in Maple can be adapted to cylindrical and spherical geometries.

Other parameters, such as the lag time and the diffusion coefficient, can also be found by combining graphical methods with the solutions developed in this work. Caution should be taken when using the notion of a time constant for a diffusive process to predict the flux. The dynamic behavior of a Fickian mechanism involves a lag time, which is not observed in linear systems described by first-order differential equations (also called first-order systems). In fact, the rate of change of the flux would be maximum at $\tau = 0$ if $J(\tau)$ could be accurately modeled as a first-order linear time-invariant system. Previous studies show that the discrepancy, when using a single time constant to predict $J(\tau)$, decreases as the delivery rate settles to a steady state [11]. As time approaches $4\tau_{eff}$, the error becomes relatively small. This observation explains why 98% of $J(\tau)$ was reached at $4\tau_{eff}$, as would be expected of linear first-order processes.

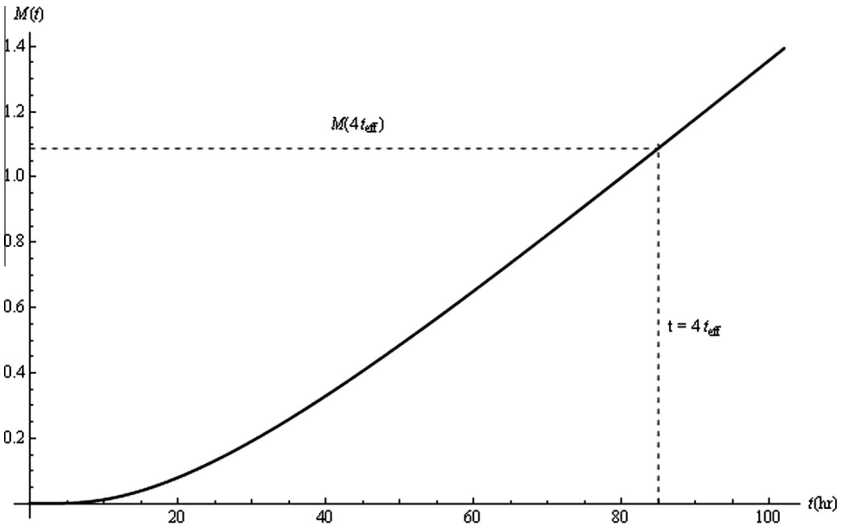

Fig. 3. Normalized cumulative amount of timolol released (M). The zero- and first-order solutions overlap. The value of M at four times the effective time constant t_{eff} is represented by dotted lines.

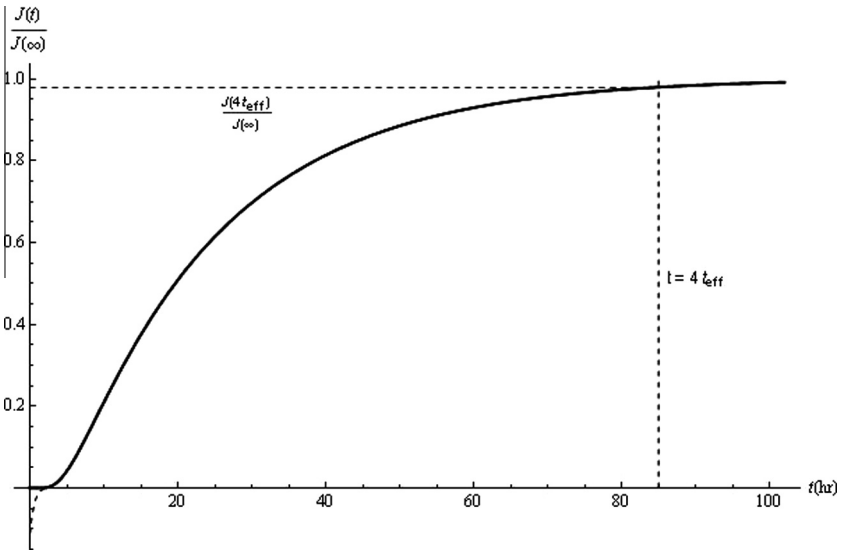

Fig. 4. Normalized timolol flux. The zero- (dotted line) and first-order approximations (solid line) were indiscernible except at very small times.

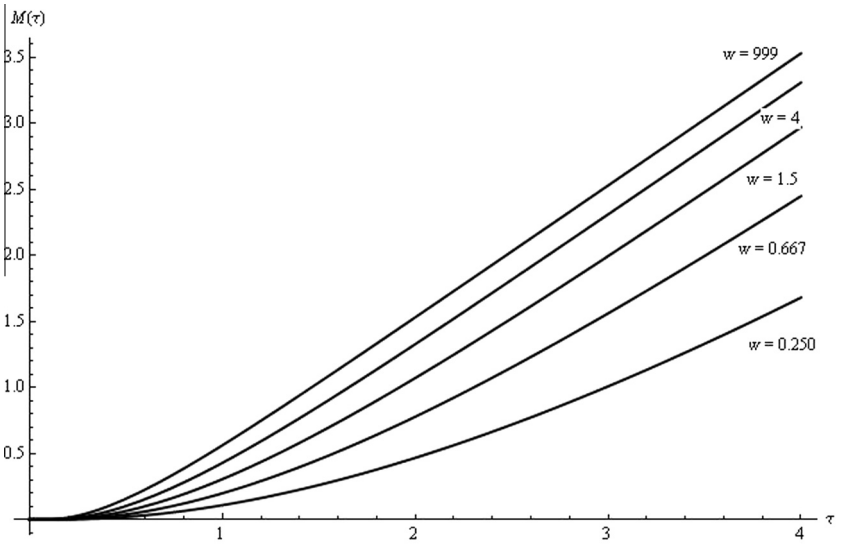

Fig. 5. Effects of $w = \frac{l_k K_d}{D}$ on the normalized cumulative amount of drug released (i.e., the inverse Laplace transform of Eq. (56)). The first-order solution was employed.

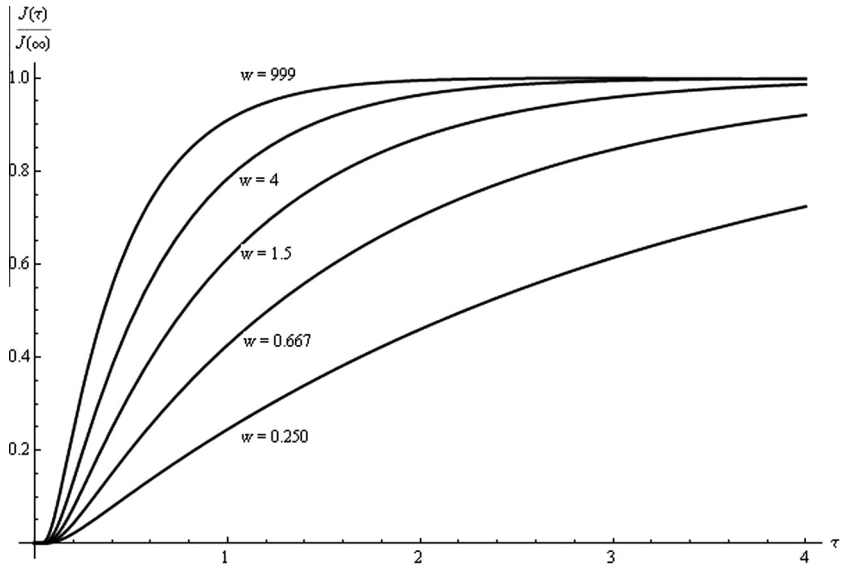

Fig. 6. Effects of $w = \frac{l_s K_{al}}{D}$ on the normalized flux, which was derived by inverting Eq. (55) and dividing the result by $J(\infty)$. This equation was developed from a first-order solution of the concentration.

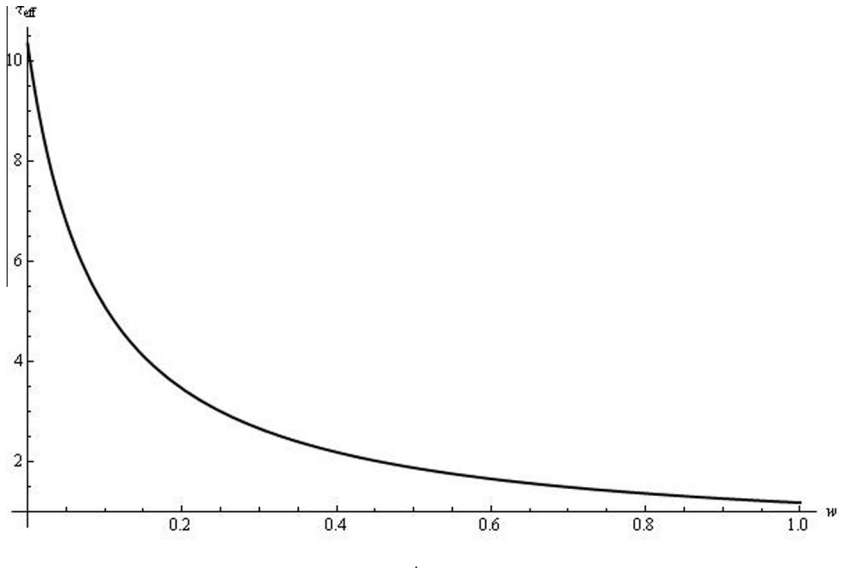

Fig. 7. Influences of $w = \frac{l_s K_{al}}{D}$ on the effective time constant τ_{eff}. The first-order solution was used.

This work can also be used to estimate the application time of a transdermal therapeutic system (TTS). Because this parameter is closely related to the time required to achieve a steady-state plasma drug concentration [12], the prediction of a time constant for a more representative 2-D model of the process is important in the field. A better description of the system dynamic behavior would help figure out when to replace patches and if continuous drug supply to the bloodstream occurs [13]. One-dimensional representations and simulations of repeated application and removal of the TTS show the use of mathematical models in estimating the number of applications before the flux of timolol reaches a steady-state value [14,15]. In addition, optimal doses necessary to achieve a desired transdermal flux were calculated [15]. The 2-D framework developed in this contribution can be extended to these cases and provide a more accurate depiction of mass transport. As manufacturers continue to develop products for percutaneous delivery, there is a growing need to develop mathematical models that capture the transport processes [16]. The derivation of a time constant, in terms of key properties of the vehicle, would help assess the performance of these new devices with a reduced number of experiments. The approach is appropriate for a range of controlled-release devices. Using 1-D models, researchers tested the time-constant method to gain insight into the effects of iontophoresis and penetration enhancers on drug transport across the oral mucosa [17] and to describe drug delivery from therapeutic contact lenses [18].

7. Conclusion

An analytical solution was derived for a percutaneous drug absorption model in two dimensions. After implementing a Laplace transform procedure, zero- and first-order approximations were computed for the concentration (C), flux (J) and cumulative amount of drug released (M). The time necessary to reach 98% of the steady-state delivery rate was calculated ($4\tau_{eff}$). Although the zero-order estimation of C only captured transport in the direction normal to the skin surface, both estimation methods led to similar values of J, M and τ_{eff}. Based on the zero-order analysis, a high clearance rate at the skin-capillary boundary would lead to a shorter relaxation time. This result agrees with published data gener-

ated using numerical methods. Simulations conducted to describe skin permeation of timolol show that J and M increased as the drug *absorption rate* increased. Advantages of the proposed approach are the development of expressions that can be adopted for design purposes and parameter estimations. Caution should be exercised when using τ_{eff} as a dynamic performance criterion. The method can be used to assess the dynamic performance of novel controlled-release systems.

Appendix A. Source code

```
> > restart:with(VectorCalculus):with(inttrans):with(PDETools):with(plots):
>
> eql:=diff(C(x,y,t),t)=Laplacian(C(x,y,t),cartesian[x,y]);
> eq2:=C(x,y,0)=0;
> Eval(diff(C(x,y,t),y),y=L[u])=0;
> lor:=Eval(diff(C(x,y,tau),x),x=0)=Eval(diff(C(x,y,tau),x)+C(x,y,tau)-l,x=0)*(Heaviside(y)-Heaviside(y-
  L[c]));
> convert(lor,piecewise,y) assuming y>0 and L[c]>0;
> Heaviside(y-a)=piecewise(y>=a,1,0);
> lor assuming y<0 and L[c]>0;
> lor assuming y>L[c] assuming y>0;
> lor assuming y>0 and y<L[c];
> Eval(diff(C(x,y,t),x)+w*C(x,y,t),x=l)=0;
> eq3:=laplace(eql,t,s);
> eq4:=subs(eq2,eq3);
> eq5:=subs(laplace(C(x,y,t),t,s)=C(x,y),eq4);
> eq6:=pdsolve(eq5,HINT=f(x)*g(y));
> eq7:=factor(build(eq6));
> eq8:=subs(y=-L[d],diff(rhs(eq7),y))=0;
> eq9:=subs(y=L[u],diff(rhs(eq7),y))=0;
> eql0:=isolate(eq8,_C4);
> eqll:=factor(subs(eql0,eq9));
> eql2:=factor(combine(cos((-s+_c[l])^(1/2)*L[u])*sin((-s+_c[l])^(1/2)*L[d])+cos((-s+_c[l])^(1/
  2)*L[d])*sin((-s+_c[l])^(1/2)*L[u]),sin))=0;
> eql3:=(-s+_c[l])^(1/2)*(L[u]+L[d])=n*Pi;
> eql4:=isolate(eql3,_c[l]);
> eql5:=simplify(subs(eql4,eql2),power,symbolic);
>
>
> eql7:=simplify(subs(eql4,eql0),power,symbolic);
> eql8:=factor(subs(eql7,eq7));
> eql9:=factor(combine(simplify(subs(_C3=1,subs(eql4,eql8)),power,symbolic)));
>
>
>
> eq23:=subs(_Cl=A[n],_C2=B[n],eql9);
> eq24:=C(x,y)=Sum(rhs(eq23),n=0..infinity);
> eq24A:=factor(subs(A[n]=A[n]*sin(n*Pi/(L[u]+L[d])*L[d]),B[n]=B[n]*sin(n*Pi/(L[u]+L[d])*L[d]),eq24));
> eq24B:=C(x,y)=eval(simplify(subs(n=0,-cos(n*Pi*(y+L[d])/
  (L[u]+L[d]))*(A[n]*exp((n^2*Pi^2+s*L[u]^2+2*s*L[u]*L[d]+s*L[d]^2)^(1/2)/(L[u]+L[d])*x)+exp(-
  (n^2*Pi^2+s*L[u]^2+2*s*L[u]*L[d]+s*L[d]^2)^(1/2)/(L[u]+L[d])*x)*B[n])),power,symbolic))+Sum(-
  cos(n*Pi*(y+L[d])/(L[u]+L[d]))*(A[n]*exp((n^2*Pi^2+s*L[u]^2+2*s*L[u]*L[d]+s*L[d]^2)^(1/2)/
  (L[u]+L[d])*x)+exp(-(n^2*Pi^2+s*L[u]^2+2*s*L[u]*L[d]+s*L[d]^2)^(1/2)/(L[u]+L[d])*x)*B[n]),n = 1 ..
  infinity);
> G[n]=sqrt(rhs(eql4));
> simplify(isolate(sqrt(n^2*Pi^2+s*L[u]^2+2*s*L[u]*L[d]+s*L[d]^2)=G[n]*(L[u]+L[d]),G[n]));
> eq24C:=subs(sqrt(n^2*Pi^2+s*L[u]^2+2*s*L[u]*L[d]+s*L[d]^2)=G[n]*(L[u]+L[d]),eq24B);
> eq25:=subs(x=l,diff(rhs(eq24C),x)+w*rhs(eq24C))=0;
> eq25A:=-A[0]*s^(1/2)*exp(s^(1/2))+s^(1/2)*exp(-s^(1/2))*B[0]+w*(-A[0]*exp(s^(1/2))-exp(-s^(1/
  2))*B[0])=0;
> eq25B:=simplify(simplify(factor(isolate(eq25A,B[0])),power,symbolic),exp);
> eq26:=-cos(n*Pi*(y+L[d])/(L[u]+L[d]))*(A[n]*G[n]*exp(G[n])-G[n]*exp(-G[n])*B[n])+w*(-cos(n*Pi*(y+L[d])/
  (L[u]+L[d]))*(A[n]*exp(G[n])+exp(-G[n])*B[n]));
> eq27:=simplify(factor(isolate(eq26,B[n])),exp);
> eq28:=(subs({eq25B,eq27},eq24C));
>
> cucal:=C(s,x,y) = simplify(factor(-A[0]*exp(s^(1/2)*x)-exp(-s^(1/2)*x)*A[0]*exp(2*s^(1/2))*(s^(1/2)+w)/
  (s^(1/2)-w)),exp)+Sum(-cos(n*Pi*(y+L[d])/(L[u]+L[d]))*simplify(factor(A[n]*exp(G[n]*x)-exp(-
  G[n]*x)*A[n]*(G[n]+w)/(-G[n]+w)*exp(2*G[n])),exp),n = 1 .. infinity);
```

References

[1] B.G. Saar, L.R. Contreras-Rojas, X.S. Xie, R.H. Guy, Imaging drug delivery to skin with stimulated Raman scattering microscopy, Mol. Pharm. 8 (2011) 969.

[2] A.L. Bunge, Release rates from topical formulations containing drugs in suspension, J. Control. Release 52 (1998) 141.

[3] K. Kubota, F. Dey, S.A. Matar, E.H. Twizell, A repeated-dose model of percutaneous drug absorption, Appl. Math. Model. 26 (2002) 529.

[4] L. Simon, N.W. Loney, An analytical solution for percutaneous drug absorption: application and removal of the vehicle, Math. Biosci. 197 (2005) 119.

[5] A.J. Lee, J.R. King, T.G. Rogers, A multiple-pathway model for the diffusion of drugs in skin, IMA J. Math. Appl. Med. Biol. 13 (1996) 127.

[6] K. George, K. Kubota, E. Twizell, A two-dimensional mathematical model of percutaneous drug absorption, Biomed. Eng. Online 3 (2004) 18.

[7] K. George, A two-dimensional mathematical model of non-linear dual-sorption of percutaneous drug absorption, Biomed. Eng. Online 4 (2005) 40.

[8] R. Collins, The choice of an effective time constant for diffusive processes in finite systems, J. Phys. D Appl. Phys. 13 (1980) 1937.

[9] L. Simon, Timely drug delivery from controlled-release devices: dynamic analysis and novel design concepts, Math. Biosci. 217 (2009) 151.

[10] K. Kubota, T. Yamada, Finite dose percutaneous drug absorption: theory and its application to in vitro timolol permeation, J. Pharm. Sci. 79 (1990) 1015.

[11] J.A. Ferreira, P. Oliveira, P. da Silva, L. Simon, Flux tracking in drug delivery, Appl. Math. Model 35 (2011) 4684.

[12] S. Farahmand, H.I. Maibach, Transdermal drug pharmacokinetics in man: interindividual variability and partial prediction, Int. J. Pharm. 367 (2009) 1.

[13] A.E. Vasil'ev, I.I. Krasnyuk, S. Ravikumar, V.N. Tockmakhchi, Drug synthesis methods and manufacturing technology, transdermal therapeutic systems for controlled drug release (A review), Pharm. Chem. J. 35 (2001) 613.

[14] K. Kubota, F. Dey, S.A. Matar, E.H. Twizell, A repeated-dose model of percutaneous drug absorption, Appl. Math. Modell. 26 (2002) 529.

[15] L. Simon, Repeated applications of a transdermal patch: analytical solution and optimal control of the delivery rate, Math. Biosci. 209 (2007) 593.

[16] Y.G. Anissimov, O.G. Jepps, Y. Dancik, M.S. Roberts, Mathematical and pharmacokinetic modelling of epidermal and dermal transport processes, Adv. Drug Deliv. Rev. 65 (2013) 169.

[17] R. Wei, L. Simon, L. Hu, B. Michniak-Kohn, Effects of iontophoresis and chemical enhancers on the transport of lidocaine and nicotine across the oral mucosa, Pharm. Res. 29 (2012) 961.

[18] J.A. Ferreira, P. Oliveira, P. da Silva, Controlled drug delivery and ophthalmic applications, Chem. Biochem. Eng. Q. 26 (2012) 331.